Computational and Theoretical Chemistry 1207 (2022) 113531

Contents lists available at ScienceDirect

Computational and Theoretical Chemistry

journal homepage: www.elsevier.com/locate/comptc

Can time-dependent double hybrid density functionals accurately predict electronic excitation energies of BODIPY compounds?

Wissam Helal *, Qabas Alkhatib, Mohammed Gharaibeh

Department of Chemistry, The University of Jordan, Amman 11942, Jordan

ARTICLE INFO

Keywords:
BODIPY
TD-DFT
Double-hybrid
Spin-component-scaled
Vertical absorption

ABSTRACT

The vertical excitation energies of 12 BODIPY chromophores are benchmarked via TD-DFT, using 36 functionals covering different rungs. It was found that most TD-DFT results overestimate the excitation energies, and provide mean absolute error (MAE) values larger than 0.4 eV. The dispersion-corrected, spin-component-scaled, double-hybrid (DSD) density functionals DSD-BLYP and DSD-PBEP86 are found to have the smallest MAE values of 0.119 eV and 0.124 eV, respectively. The low MAE values of the two DSD density functionals falls in the range of errors found in the wavefunction based methods that are reported to be suitable methods for such chromophores. DSD-BLYP and DSD-PBEP86 functionals also show excellent consistency (standard deviation = 0.076 eV and 0.082 eV respectively) and good predictability (linear determination coefficient R^2 = 0.933 eV and 0.917 eV respectively). MAE values of the two spin-component-scaled DH functionals of vertical fluorescence calculations are also promising (MAE around 0.12 eV).

1. Introduction

Boron dipyrromethenes (BODIPYs) are small π conjugated chromophores with attractive optical properties [1–3]. BODIPYs exhibit high molar extinction coefficients and fluorescence quantum yields, show strong absorption and emission throughout the UV–vis region and sometimes towards the near-IR region, and possess relatively long excited-state lifetimes. These optical properties can be easily "fine-tuned" by chemical modifications through substiution variations [4–7]. Moreover, BODIPYs have excellent chemical, photo-chemical, and thermal stability. Due to their remarkable properties BODIPYs are used in many applications such as dye-sensitized solar cells (DSSC) [8–16], heterojunction organic solar cells [17–19], perovskite solar cells [20], optoelectronics and OLEDs [21,22], and in biomedical and bioimaging applications [23–25]. In addition, BODIPYs molecular structures are ideal models to test and benchmark theoretical methods dedicated for of excited state calculations.

Given the experimental significance of BODIPYs, many theoretical and computational studies and benchmarks have been carried out to understand their interesting excited states properties [26–40]. These benchmarks and studies tested different calculation methods and regimes: "Pure" time-dependent density functional theory (TD-DFT) in terms of vertical absorption [26,27] and E_{0-0} values [28–30]; "combined" TD-DFT such as combined TD-DFT and SOS-CIS(D) [31–33], combined TD-DFT and Bethe–Salpeter formalism [34], and spin-flip TD-DFT approach [35]; and *ab initio* methods such as many different implementations of coupled-cluster method [27,36–40]. Despite these and many other studies, the photophysics of BODIPYs is still not yet fully understood, and the accurate calculation of the excited-state properties of BODIPY and other cyanine-like chromophores is still a great challenge for quantum chemical methods.

In reality, conventional TD-DFT is the method of choice when studying electronic excited states (ES) for most compounds; this is due to its accuracy for excitation energies (errors in the range 0.1–0.3 eV) for many molecular systems, and efficiency in terms of the calculation time and the molecular sizes that can be practically treated with such a simple and straightforward regime. Nevertheless, TD-DFT highly overestimates the low-lying ES of BODIPYs. The problem of TD-DFT with BODIPY, and potentially other cyanine-like chromophores, is thought to be due to 1) a poor description of charge transfer, 2) the single reference nature of TD-DFT, and 3) the particular nature of BODIPY and other cyanine-like dyes where double excitations play a very important role [41,42,27,33]. Momeni and Brown showed that the charge transfer in the BODIPYs examined in a bencmark set of 17 small compound cannot be the major source of error in TD-DFT [27]. Actually, they have found that the problems with TD-DFT arise from difficulties in dealing with the

* Corresponding author.
E-mail address: wissam.helal@ju.edu.jo (W. Helal).

https://doi.org/10.1016/j.comptc.2021.113531
Received 7 October 2021; Received in revised form 9 November 2021; Accepted 24 November 2021
Available online 29 November 2021

differential electron correlation and from contributions of double excitations. In particular, they applied the T_1 [43] and the %TAE[T] [44] diagnostic tests and found no multireference nature for the BODIPY compounds investigated in their set. In fact, using the CI eigenvectors of CASSCF calculations, they have found that the double excitations play a significant role in the excited states of BODIPY compounds. In fact, the importance of double excitations was also indicated previously for BODIPY compounds [45] and for cyanine dyes in general [41,42,33].

While TD-DFT suffers from many presumably problems concerning ES property calculations of BODIPYs, many studies demonstrated that some *ab initio* methods or combined TD-DFT and *ab initio* procedures perform reasonably well [27,31–34,38]. For instance, Momeni and Brown found that the mean absolute error (MAE) of the Laplace transformed local CC2 (LCC2*), the symmetry adapted cluster-configuration interaction (SAC-CI), and CASPT2 ranges between 0.1 to 0.15 eV [27,38]. Moreover, Feldt and Brown investigated the newly implemented DLPNO-STEOM-CCSD method [39,40], and found similar promising MAE values [38]. In fact, combined TD-DFT/*ab initio* regimes also shows excellent performance for 0–0 energies with errors in the range 0.1–0.2 eV, when TD-DFT is corrected with vertical CIS(D) and SOS-CIS(D) [31–33], Bethe–Salpeter formalism [34], or the spin-flip TD-DFT approach [35]. However, when it comes to the vertical excitation energies of BODIPY chromophores, no "pure" TD-DFT functional can perform as good as those wavefunction based or combined methods. Typical errors using TD-DFT for BODIPY chromophores are usually more than 0.3 eV [29,27].

Double hybrid (DH) functionals are implemented by mixing generalized gradient approximations (GGAs) for exchange and correlation with Hartree–Fock (HF) exchange and a perturbative second-order correlation part [46–48]. DH functionals are increasingly used in TD-DFT calculations [49–54]. TD using Double hybrids are, however, not extensively investigated for BODIPY and other cyanine-like chemical systems [41]. We have therefore decided to investigate the performance of DH functionals for the theoretical prediction of the vertical excitations and emmisions of a certain set of BODIPY chromophores. In particular, we have benchmarked the following DH functionals using TD-DFT: B2PLYP [46], B2GPPLYP [55], mPW2PLYP [56], the empirical dispersion-corrected, spin-component-scaled, double-hybrid (DSD) functionals (DSD-BLYP and DSD-PBEP86) [57,58], and the range separated DH functionals ωB2PLYP and ωB2GPPLYP [52]. We have also tested the performance of TD-DFT using 29 other functionals from otehr rungs (see the Computational Methods for details). The benchmark set that we have selected includes 12 BODIPY molecules of moderate size, named **I** to **XII**; see Fig. 1.

2. Computational methods

All quantum chemical calculations have been carried out with ORCA 4.2.0 code [59,60], and cube files were generated using ORCA 4.2.0 utility program orca_plot [59]. Molecular orbital isosurface densities have been visualized using Gabedit 2.4.8 [61]. The ground state (GS) equilibrium geometries of all molecules have been fully optimized without any symmetry restriction using DFT employing PBE0 functional [62] and the Ahlrichs def2-TZVP [63] basis set. PBE0 functional has been shown to produce accurate ground state geometries for BODIPY based molecules [26]. The excited state (ES) geometries were optimized with TD-DFT using the CAM-B3LYP functional as suggested by the benchmark studies of Jacquemin et al. [64,65]. In addition, subsequent frequency calculations were carried out for all optimized geometries at the same level of theory (PBE0/def2-TZVP for GS geometries and CAM-B3LYP/def2-TZVP for ES geometries) in order to test the nature of the stationary points. Only real frequency values for equilibrium state structures were accepted.

The lowest 20 singlet–singlet vertical electronic excitations of the optimized GS geometries were computed for all molecules by means of TD-DFT using 36 different functionals, discussed *vide infra*, with def2-TZVP basis set. The Tamm-Dancoff approximation (TDA), which is set as default in TD-DFT ORCA module, was not used in all TD-DFT calculations. In the case of fluorescence calculations, the lowest 20 singlet–singlet vertical electronic excitations based on CAM-B3LYP optimized ES geometries were computed for all molecules by means of TD-DFT using the 7 double hybrid functionals. We have assessed the impact of solvent effects in all geometry optimizations of the ground state using the linear-response (LR) conductor-like polarizable continuum model (CPCM) [66], and solvents as indicated by the corresponding experimental results. ES geometry optimizations were all performed in vacuum. In addition, solvent effects were also considered for all vertical absorption and fluorescence transitions of the relaxed structures at the TD-DFT/def2-TZVP level, with the same solvation model and solvent as that for the geometry optimization step. The solvent used in geometry optimizations and single point vertical excitation energies is the same as that used in the experimental determination of the UV–vis absorption

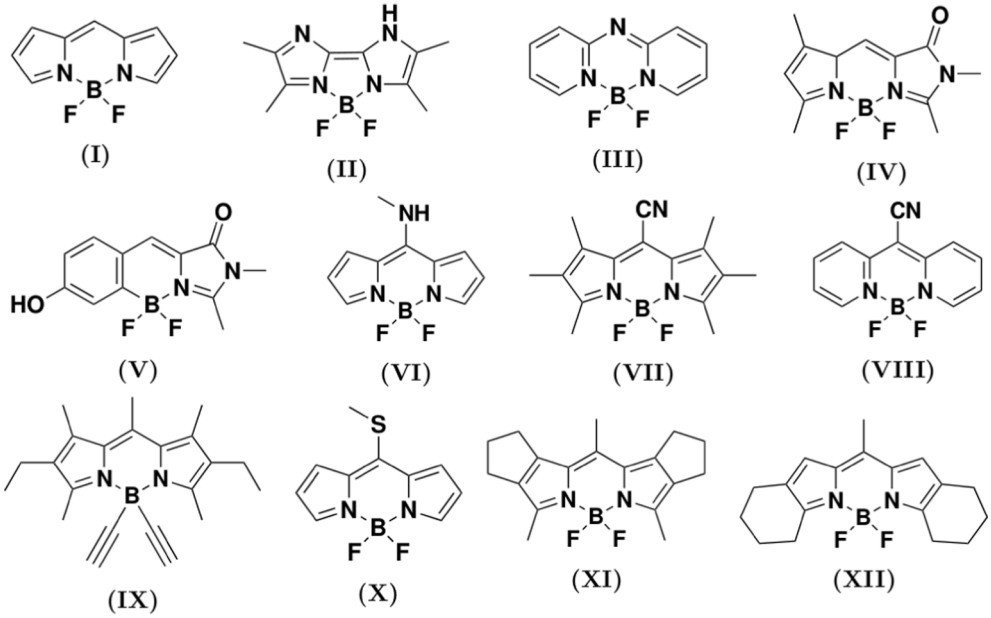

Fig. 1. The molecular structure of BODIPY compounds considered in this study.

spectra, see Table 1. Gas phase excited state calculations were also considered for all molecules using all functionals.

All DFT/TD-DFT calculations were sped up with the resolution-of-the-identity (RI) approximation. The RIJCOSX procedure [67], a standard setting in ORCA which uses both the RI approximation for Coulomb integrals (RI-J) and the chain-of-spheres approximation for exchange integrals (COSX) [68], is employed with all functionals. Moreover, the RI-MP2 [69] is also used for the DH and RSDH functionals. The corresponding auxiliary basis sets were used: the def2/J basis set for RIJCOSX [70] and the def2-TZVP/C for RI-DH [71]. Converged SCF orbitals were obtained using the TightSCF setting in ORCA (energy change $= 10^{-8}\ E_h$). A multi-grid approach [72] for the numerical quadrature integration was chosen, where the SCF iterations are done with a given grid whereas gradients and final energies are evaluated on a larger more accurate grid. In particular, ORCA's multigrid "grid5 finalgrid6 gridx6" was used, which consists of a pruned grid of 40 radial shells (GaussChebyshev) and 434 angular points (Lebedev434) per shell during the SCF iterations, and a pruned grid of 45 radial shells and 590 angular points per shell for the final energy after SCF convergence, with the COSX grid settings "gridx6".

We have investigated the performance of 36 functional: 8 generalized gradient approximation (GGA), 2 meta-GGA (mGGA), 8 global-hybrid GGA (GH-GGA), 4 global-hybrid meta-GGA (GH-mGGA), 7 range separated hybrid GGA (RSH-GGA), 5 double hybrid GGA (DH-GGA), and 2 range separated double hybrid GGA (RSDH-GGA). A complete list of functionals considered in this work is given in Table 2. The exchange correlation (xc) energy E_{xc} of a global hybrid GGA (E_{xc}^{GH-GGA}), has the general form:

$$E_{xc}^{GH-GGA} = a_x E_x^{HF} + (1-a_x)E_x^{GGA} + E_c^{GGA} \quad (1)$$

where the scaling parameter a_x governs the fraction of E_x^{HF} in the hybrid functional, E_x^{HF} is the Hartree–Fock exchange energy expression, and E_x^{GGA} and E_c^{GGA} are the DFT exchange and correlation energy density functional approximations, respectively. In double-hybrid (DH) functionals, nonlocal wavefunction type terms substitute parts of semi-local DFT components, for both the exchange (x) and the correlation (c) energy. In its simplest form, as introduced by Grimme in 2006 [46], the DH-GGA xc-energy expression (E_{xc}^{DH-GGA}) is:

$$E_{xc}^{DH-GGA} = (1-a_x)E_x^{DFT} + a_x E_x^{HF} + (1-a_c)E_c^{DFT} + a_c E_c^{MP2} \quad (2)$$

where E_c^{MP2} is a nonlocal second-order perturbative correlation-energy term, and a_x and a_c are scale parameters. TD-DFT DH functionals use a CIS(D) like perturbative correction for the TD-DFT energies. Details of calculation procedures for time-dependent DH functionals are found in the literature [41,49]. The general form of the dispersion-corrected, spin-component-scaled, double-hybrid (DSD) functionals is [57]:

$$E_{xc}^{DSD-DFT} = (1-a_x)E_x^{DFT} + a_x E_x^{HF} + c_c E_c^{DFT} + c_o E_c^{OS-MP2} + c_s E_c^{SS-MP2} \quad (3)$$

where E_c^{OS-MP2} and E_c^{SS-MP2} are the opposite- and same-spin contributions to the MP2 energy, scaled by the parameters c_o and c_s. The scale factor c_c for the DFT correlation is independent from the two MP2 parameters.

3. Results and Discussion

All of the of 12 molecules selected as the benchmark set in this investigation (see Fig. 1) were the subject of the previous study by Momeni and Brown [27]. We have excluded five molecules from their 17 compounds set, which are (according to the numbering in their article): **2**, **3**, **4**, $\mathbf{5}_H$, and **9**. Molecules **2**, **3**, $\mathbf{5}_H$, and **9** are excluded from our study since there are no published experimental absorption spectra for these compounds. In fact, Momeni and Brown considered the theoretical CASPT2 results in the gas phase for these four compounds as a reference for benchmarking the different methods in their study. Molecule **4** is excluded from our study since all the TD-DFT results were outliers when compared with experimental results. Actually, Momeni and Brown reported two MAE values, one including the results of molecule **4**, and one excluding them. In the following, we have always compared our MAE values with their values where molecule **4** is excluded. In addition, the present study is concerned with vertical excitations or emissions [73,27,38], which, in fact, cannot always be directly compared to experimental absorption or fluorescence maxima, since the vibronic effects are not considered in such a simple procedure. On the other hand, E_{0-0} can be directly compared with the experimental absorption-fluorescence crossing point (AFCP). It has been shown, however, that the use of the vertical approximation is justified in the case of BODIPY compounds [27]. As a matter of fact, temperature variations may lead to shifts in the absorption and emission maxima. However, we did not consider temperature effects on the ES calculations of our set of molecules, since our vocus is on vertical excitations as previously justified.

The mean absolute error (MAE), the relative maximum error (Max), the relative minimum error (Min), the standard deviation (SD), and the linear determination coefficient R^2, of the computed TD-DFT vertical absorption energies for all functionals in both the gas phase and solvent are reported in Table 3. Details of TD-DFT vertical absorption energies for all functionals and all BODIPY compounds in the gas phase and in solvent are reported in the supplementary material S1 – S10.

The results of vertical absorption energies in both the gas phase and solvent are found to be similar for many functionals and even almost identical for some other functionals; as listed in Table 3. For instance, the mean absolute error (MAE) values for the GGA functionals in the gas phase are around 0.02 eV higher than that in solvent, while the difference becomes around 0.03 eV for the GH-GGA functionals and around 0.04 eV for mGGAs and GH-mGGAs. It is worthwhile to note that the MAE of the gas phase calculations using the range separated functionals RSH-GGA and RSDH-GGA are around 0.02 eV lower than that in solvent. Moreover, the three DH functionals B2PLYP, B2GPPLYP, and mPW2PLYP give almost identical vertical absorption energy MAE values

Table 1
Experimental Maximum Absorption and Fluorescence Values (eV) Used as Reference in This Study, and the Corresponding Solvents Used in Experiment.

	Absorption	Fluorescence	Solvent	Reference
I	2.460	2.407	cyclohexane	[76]
II	3.712	3.289	dichloromethane	[77]
III	3.125	3.112	tetrahydrofuran	[78]
IV	2.583	2.525	dichloromethane	[79]
V	2.995	2.605	dichloromethane	[80]
VI	2.963	2.678	cyclohexane	[81]
VII	2.109	2.026	ethanol	[82]
VIII	2.755	2.719	hexane	[83]
IX	2.412	2.322	dichloromethane	[84]
X	2.353	2.300	methanol	[85]
XI	2.422	2.317	ethanol	[86]
XII	2.317	2.214	ethanol	[86]

Table 2
List of functionals used in this work, arranged according to their type.

Functional	a_x (% HF)	a_c	c_c	c_o	c_s	ω bohr^{-1}	exchange functional	correlation functional	Year	Ref
GGA										
OLYP							OptX	LYP	2001	[87,88]
BLYP							B88	LYP	1988	[89,87]
BP86							B88	P86	1988	[89,90]
XLYP							B88 + PW91	LYP	2004	[87,91]
PBE							PBE(X)	PBE(C)	1996	[92]
mPWPW							mPW91	PW91	1998	[93]
mPWLYP							mPW91	LYP	1998	[93,87]
B97-D3							RB97	B97	2011	[94]
mGGA										
M06-L							M06-L(X)	M06-L(C)	2006	[95]
TPSS							TPSS	TPSS	2003	[96]
GH-GGA										
O3LYP	11.6						OptX	LYP	2001	[87,88]
B3LYP	20						B88	LYP	1993	[97,98]
B3P86	20						B88	P86	1993	[97,90]
X3LYP	22						B88 + PW91	LYP	2004	[87,91]
PBE0	25						PBE(X)	PBE(C)	1999	[62]
mPW1PW	25						mPW91	PW91	1998	[93]
mPW1LYP	25						mPW91	LYP	1998	[93,87]
BH&HLYP	50						B88	LYP	1993	[99]
GH-mGGA										
TPSSh	10						TPSS	TPSS	2003	[100]
TPSS0	25						TPSS	TPSS	2005	[101]
M06	27						M06(X)	M06(C)	2008	[102]
M06-2x	54						M06-2X(X)	M06-2X(C)	2008	[102]
RSH-GGA										
LC-BLYP	0–100					0.33	B88	LYP	2004	[103]
CAM-B3LYP	19–65					0.33	B88	LYP	2004	[104]
ωB97	0–100					0.40	ωB97	B97	2008	[105]
ωB97X	15.77–100					0.30	ωB97X	B97	2008	[105]
ωB97X-D3	19.57–100					0.25	ωB97X	B97	2013	[106]
ωB97X-D3(BJ)	16.7–100					0.30	ωB97X	B97	2018	[107]
ωB97X-V	16.7–100					0.30	ωB97X	B97	2014	[108]
DH-GGA										
B2PLYP	0.53	0.27					B88	LYP	2006	[46]
B2GPPLYP	0.65	0.36					B88	LYP	2008	[55]
mPW2PLYP	0.55	0.25					mPW	LYP	2006	[56]
DSD-BLYP	0.69		0.54	0.46	0.37		B88	LYP	2010	[57]
DSD-PBEP86	0.70		0.43	0.53	0.25		PBE	P86	2011	[58]
RSDH-GGA										
ωB2PLYP	0.53	0.27				0.30	ωB88	LYP	2019	[52]
ωB2GPPLYP	0.65	0.36				0.27	ωB88	LYP	2019	[52]

List of abbreviations and symbols: **GGA**: generalized gradient approximation; **mGGA**: meta-GGA; **GH**: global hybrid; **RSH**: range separated hybrid; **DH**: double hybrid; **RSDH**: range separated double hybrid; a_x: scale factor for exact (HF) exchange in GH-GGA [Eq (1)], GH-mGGA, RSH-GGA, DH-GGA [Eq (2)], and RSDH-GGA; a_c second-order perturbative correlation for various DH-GGA [Eq (2)]; c_c, c_o, and c_s: scale factors of the DFT correlation, perturbative correlation contribution of opposite-spin electron pairs and that of same-spin electron pairs, respectively, for the DSD functionals [Eq (3)]; and ω: screening factor (for RSH and RSDH functionals).

Table 3
The Mean Absolute Error (MAE), Relative Maximum Error (Max), Relative Minimum Error (Min), Standard deviation (SD), and Linear Determination Coefficient (R^2) of BODIPY's Vertical Excitation Energies (eV) Using all Functionals with the def2-TZVP Basis Set in the Gas Phase and in Solvent.

	MAE		Max		Min		SD		R^2	
Functional	Gas	Solv	Gas	Solv	Gas	Solv	Gas	Solv	Gas	Solv
GGA										
OLYP	0.297	0.277	0.594	0.542	0.008	0.051	0.192	0.154	0.835	0.768
BLYP	0.273	0.253	0.561	0.507	0.025	0.003	0.182	0.149	0.826	0.762
BP86	0.280	0.260	0.574	0.522	0.010	0.013	0.188	0.154	0.827	0.763
XLYP	0.272	0.253	0.559	0.506	0.027	0.005	0.181	0.148	0.826	0.762
PBE	0.280	0.260	0.575	0.523	0.012	0.010	0.188	0.154	0.825	0.761
mPWPW	0.281	0.261	0.575	0.523	0.010	0.016	0.188	0.153	0.828	0.762
mPWLYP	0.270	0.252	0.559	0.506	0.027	0.010	0.181	0.147	0.823	0.759
B97-D3	0.296	0.275	0.590	0.534	0.008	0.045	0.190	0.153	0.834	0.768
mGGA										
M06-L	0.437	0.383	0.717	0.661	0.140	0.031	0.181	0.197	0.866	0.799
TPSS	0.346	0.311	0.637	0.584	0.042	0.049	0.192	0.174	0.846	0.784
GH-GGA										
O3LYP	0.408	0.360	0.683	0.635	0.084	0.005	0.176	0.192	0.879	0.837
B3LYP	0.461	0.427	0.712	0.676	0.154	0.091	0.158	0.169	0.906	0.881
B3P86	0.473	0.439	0.723	0.687	0.173	0.109	0.156	0.168	0.906	0.880
X3LYP	0.473	0.442	0.720	0.687	0.170	0.109	0.154	0.165	0.910	0.886
PBE0	0.513	0.485	0.749	0.724	0.232	0.175	0.145	0.155	0.915	0.895
mPW1PW	0.513	0.486	0.748	0.723	0.232	0.173	0.144	0.155	0.916	0.895
mPW1LYP	0.494	0.467	0.733	0.705	0.198	0.141	0.148	0.157	0.916	0.896
BH&HLYP	0.641	0.643	0.807	0.835	0.439	0.410	0.112	0.124	0.937	0.924
GH-mGGA										
TPSSh	0.448	0.402	0.715	0.668	0.144	0.070	0.171	0.187	0.884	0.846
TPSS0	0.556	0.532	0.783	0.761	0.290	0.235	0.138	0.149	0.921	0.902
M06	0.438	0.416	0.670	0.653	0.137	0.083	0.142	0.154	0.924	0.902
M06-2x	0.559	0.556	0.716	0.740	0.406	0.411	0.103	0.109	0.947	0.941
RSH-GGA										
LC-BLYP	0.548	0.560	0.696	0.757	0.450	0.416	0.103	0.114	0.952	0.942
CAM-B3LYP	0.564	0.563	0.741	0.768	0.373	0.350	0.109	0.118	0.942	0.931
ωB97	0.614	0.635	0.814	0.828	0.476	0.437	0.120	0.132	0.954	0.945
ωB97X	0.603	0.618	0.772	0.800	0.494	0.453	0.109	0.120	0.950	0.940
ωB97X-D3	0.595	0.604	0.746	0.796	0.463	0.454	0.107	0.117	0.945	0.936
ωB97X-D3(BJ)	0.632	0.646	0.802	0.829	0.518	0.480	0.110	0.121	0.949	0.940
ωB97X-V	0.632	0.646	0.802	0.829	0.518	0.480	0.110	0.121	0.949	0.940
DH-GGA										
B2PLYP	0.400	0.400	0.593	0.591	0.181	0.175	0.115	0.109	0.954	0.955
B2GPPLYP	0.420	0.430	0.587	0.607	0.249	0.255	0.092	0.088	0.966	0.965
mPW2PLYP	0.433	0.435	0.619	0.625	0.223	0.217	0.108	0.105	0.955	0.955
DSD-BLYP	0.134	0.119	0.277	0.238	-0.169	-0.147	0.088	0.076	0.910	0.933
DSD-PBEP86	0.145	0.124	0.271	0.231	-0.215	-0.194	0.095	0.082	0.886	0.917
RSDH-GGA										
ωB2PLYP	0.519	0.542	0.662	0.710	0.406	0.406	0.094	0.106	0.963	0.956
ωB2GPPLYP	0.499	0.524	0.629	0.687	0.387	0.400	0.088	0.101	0.967	0.959

for both the gas phase and solvent. However, the mean absolute errors of the TD calculations in solvent for DSD-BLYP and DSD-PBEP86 functionals are 0.015 and 0.021 eV lower than that in the gas phase, respectively. As for the relative maximum error (Max) values, most vertical excitation results in solvent are lower than that in the gas phase by a range of 0.015–0.055 eV, except for the RSH-GGA and RSDH-GGA functionals, where the gas phase Max values are lower than that in solvent. We have also observed a slightly better standard deviation values for the GGA and the DH-GGA functionals in solvent than the same calculations done in vacuum. Finally, most functionals show slightly lower linear determination coefficient (R^2) values in solvent as compared to the gas phase results, with the exception of DH functionals, where R^2 values in solvent are either slightly better, as the case of DSD-BLYP and DSD-PBEP86 functionals, or almost equal to that of the gas phase, as for B2PLYP, B2GPPLYP, and mPW2PLYP functionals. For example, the R^2 values for the DSD-BLYP functional in the gas and solvent phases are 0.910 and 0.933, respectively; while that for the DSD-PBEP86 functional in the gas and solvent phases are 0.886 and 0.917, respectively.

We can therefore conclude that the enhancement gained using the "standard" LR-CPCM solvation model in the case of BODIPY compounds is not significant for most functionals in general. This is in line with the conclusions made by Momeni et al. using the LR-PCM model [27] and by Chibani et al. using the corrected linear-response (cLR) and state-specific (SS) PCM solvation models [74,30]. However, it could be also concluded from our results that using the LR-CPCM solvation model could give a slight improvement in terms of consistency and predictability over gas phase calculations when using the empirical double hybrid functionals DSD-BLYP and DSD-PBEP86. We will therefore use the solvent results in the following for discussing the performance of different functionals.

In general, the prediction of vertical excitations using TD-DFT, produce typical errors in the range 0.2 – 0.4 eV for "well-behaved" molecules [75]. Methods designed for the calculation of electronic excitation energies are said to be "accurate", if the errors where close to or less than 0.1 eV. Most functionals investigated in this work, in particular GH-GGA, GH-mGGA, RSH-GGA, and RSDH-GGA functionals, have MAE values greater than 0.4 eV; see Table 3 and Fig. 2. Although range separated functionals should in principle have a good general performance for these compounds, we have found that RSH and RSDH functionals show the highest MAE values (around 0.5 – 0.6 eV). The recently proposed time-dependent DH functionals with correct asymptotic long-range behavior ωB2PLYP and ωB2GPPLYP [52], were optimized and designed for excited-state properties, unlike the other five DH functionals tested in this study that have in common being optimized and designed for ground-state applications. Nevertheless, the MAE value for these two functionals is $\sim$0.5 eV. Interestingly, the simplest GGA functionals shows MAE values in the range 0.25 – 0.30 eV, i.e. within the typical TD-DFT range of errors. The MAE values of mGGA functionals considering solvent effects were slightly higher than that of pure GGAs. The acceptable performance of GGA functionals is probably due to systematic error cancellation. In fact, these conclusions are in line with that previously obtained by Momeni and Brown [27]. Moreover, many double hybrid (DH-GGA) functionals, such as B2PLYP, B2GPPLYP, and mPW2PLYP, have MAE values of at least 0.4 eV.

From all the functionals investigated in this study, only two of them reach the desired chemical accuracy: the DH-GGA functionals DSD-BLYP (MAE = 0.119 eV) and DSD-PBEP86 (0.124 eV); see Table 3. No other functional, including other DH functionals, is similar or even close to the excellent performance of the two DSD functionals. The next lowest MAE values in solvent are that of GGA functionals, in particular BLYP (0.253 eV), XLYP (0.253 eV), and mPWLYP (0.252 eV). However, the "best" GGA functionals have almost twice the the value of mean absolute errors as that of the two DSD functionals. Actually, the low MAE values of DSD-BLYP and DSD-PBEP86 functionals are comparable with that of the wavefunction based *ab initio* methods. For instance, Momeni and Brown have found the following MAE values of the vertical excitation energy in the gas phase using cc-pVDZ: LCC2* = 0.109 eV; SAC-CI = 0.154 eV; and CASPT2 = 0.100 eV, while the LCC2* MAE value using cc-pVTZ was found to be 0.100 eV [27]. Feldt and Browm also benchmarked the DLPNO-STEOM-CCSD and found MAE values of 0.146 and 0.114 using cc-pVDZ and cc-pVTZ, respectively [38]. No other known DFT functional for BODIPY chromophores is accurate as the two DSDs tested in this work.

It is worth to notice that the low MAE values obtained for the TD-DFT in solvent using the DSD-BLYP and the DSD-PBEP86 functionals are independent of the nature of both the exchange functional (B88 in the case of DSD-BLYP and PBE in the case of DSD-PBEP86) and the correlation DFT functional (LYP in the case of DSD-BLYP and P86 in the case of DSD-PBEP86), but is probably the result of the use of the spin-component-scaled (SCS) procedure in this type of functionals. Indeed, states of double-excitation, that characterize the absorption transitions in BODIPYs, cannot be properly described in a "single-particle-based theory" such as TD-DFT, hence the general shortcomings of linear-response time-dependent DFT in the description of the excited states of these chromophores. In our case, some double-hybrid functionals

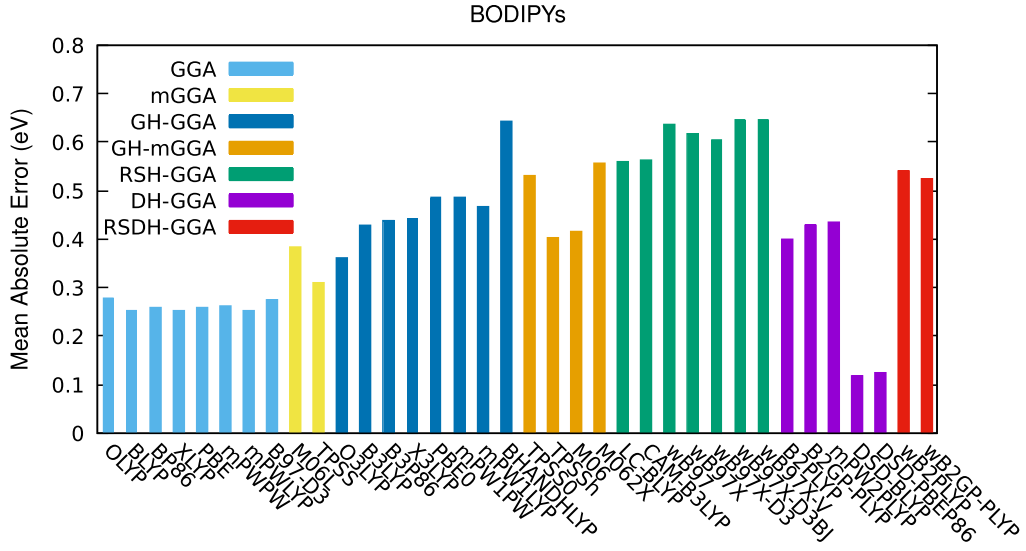

Fig. 2. Histogram showing the mean absolute error (MAE) in eV for BODIPYs using TD-DFT in solvent.

used in this study, namely B2PLYP, B2GPPLYP, and mPW2PLYP, that use CIS(D) like perturbative correction for the TD-DFT energies, did not improve the description of states presenting a double-excited nature. On the other hand, the spin-component-scaled (SCS) variation to the CIS(D), that is only found the the two DSD functionals, seems to capture these ubiquitous double excitations in BODIPY compounds.

Not only the two double hybrid DSD functionals are relatively accurate in terms of the mean absolute error values when compared to other functionals, but they have also a very good consistency and predictability. The standard deviation values of DSD-BLYP and DSD-PBEP86 in solvent are 0.076 eV and 0.082 eV, respectively. It is found that the SD values of the two DSD functionals are the lowest among all other functionals from all rungs, including other DH functionals (Table 3). The SD values for GGA, mGGA, GH-GGA, and GH-mGGA are around 0.15 eV, while they are slightly better for RSH-GGA (around 0.12 eV) and DH/RSDH functionals (around 0.1 eV). The linear determination coefficient values R^2 DSD-BLYP and DSD-PBEP86 functionals in solvent are 0.933 eV and 0.917 eV, respectively. The R^2 values of most GGA, mGGA, GH-GGA, and GH-mGGA functionals fall in the range around 0.76 – 0.89 eV, with two exceptions: the GH-GGA BH&HLYP (0.924 eV) and the GH-mGGA M06-2X (0.941 eV). However, the R^2 values of all RSH-GGA functionals (around 0.94 eV) and other DH and RSDH (around 0.96 eV) have a slightly better predictability than the two DSD functionals if they are scaled appropriately.

Furthermore, DSD-BLYP and DSD-PBEP86 functionals show the best relative maximum error: 0.238 eV and 0.231 eV, respectively. All other functionals, including DH and RSDH, have Max values in the range 0.5 – 0.8 eV (Table 3). The relative minimum error of DSD-BLYP and DSD-PBEP86 are –0.149 eV and –0.194 eV, respectively. TD-DFT vertical absorption energies for all BODIPY compounds using DH-GGA and RSDH-GGA functionals in the gas phase and in solvent are reported in Tables S9 and S10, respectively. As expected, there is an observed blue shift (hypsochromic shift) for the TD-DFT excitation energies with respect to the experimental data for the DH and RSDH functionals considered, except for the two DSD functionals (DSD-BLYP and DSD-PBEP86) for compounds **II**, **III**, **V**, and **VIII**, in which a red shift (bathochromic shift) was observed in the calculated TD-DFT, hence, a negative Min values for DSD-BLYP and DSD-PBEP86.

It is interesting to check the performance of different functionals as a function of the percentage of HF exchange. In general, hybrid DFT functionals should improve the description of charge localization in molecules. It is found that the quality, in terms of MAE, of a GH-GGA and a GH-mGGA functional, is inversely proportional to the percentage of the HF exchange (a_x), as shown in Tables 2 and 3 and Fig. 2 (in Table 3 and Fig. 2, the GH-GGA and GH-mGGA functionals are ordered according to their a_x value in an ascendant manner). The MAE value for GH-GGA functionals ranges from 0.36 eV for the O3LYP functional ($a_x = 11.6$) to 0.64 eV for the BH&HLYP functional ($a_x = 50$). A similar trend is also found for the GH-mGGAs, with the exception of TPSS0. The percentage of HF exchange is apparently irrelevant in the performance of RSH-GGA, DH-GGA, and RSDH-GGA. The screening factor ω in the RSH and RSDH functionals seems to be irrelevant for their performance as well. It is noted, however, that the RSH ωB97 functionals produce the worst MAE values, together with the BH&HLYP functional, ranging around 0.6 – 0.65 eV, with probably no benefit of the dispersion corrections found in these functionals. Finally, no clear conclusions can be made about the effect of the fraction of the second-order perturbative correlation (a_c) or other scale factors c_c, c_o, and c_s on the quality of MAE values of DH and RSDH functionals.

An analysis of the nature of the transition for the seven DH functionals are reported in Tables S14 – S20. The absorption maxima of all compounds are related to the $S_0 \rightarrow S_1$ transition, characterized by the excitation from the HOMO to the LUMO, which correspond to $\pi \rightarrow \pi^*$ transitions (Tables S14 – S20 and Figure S1). The relatively high oscillator strengths calculated for these molecules (in the range around 0.4 – 0.6; see Tables S14 – S20, reproduce in principle the high molar absorption coefficients of these compounds, which is an important characteristic of BODIPY compounds in general.

In order to investigate the performance of DH functionals in terms fluorescence spectra, we have optimized the excited state geometries of all compounds and perform TD-DFT calculations on these geometries, in gas and solvent. The results of the vertical fluorescence are presented in Table S11 for the vacuum case and in Table S12 for the solvated case. All maximum emission peaks correspond to $S_1 \rightarrow S_0$ transition and mainly contributed by the electronic transitions from LUMO to HOMO. In fact, a similar range of errors is reproduced as that of the calculated vertical excitation energies. The fluorescence MAE values of the DH functionals B2PLYP, B2GPPLYP, and mPW2PLYP in solvent are 0.335, 0.351, and 0.337, respectively. The mean absolute errors of fluorescence using the two RSDH functionals ωB2PLYP and ωB2GPPLYP are 0.471 and 0.453, respectively. As in the electronic excitation case, those two RSDH functionals gives MAEs beyond the accepTable 0.4 eV range. Finally, the two DSD functionals reproduce the most accurate emissions when compared to experiment, with MAE values around 0.12 eV for both functionals. The standard deviation and the the R^2 values for fluorescence in gas and solvent, are not promising as that of the corresponding absorption. For example, the fluorescence SD and R^2 of DSD-BLYP in solvent are 0.110 and 0.805, respectively, compared to 0.076 and 0.933, respectively, for the absorption case using the same functional in solvent. We found a similar trend for other DH and RSDH functionals.

The differences between the absorption and emission energies, i.e. the Stokes shifts, calculated at the DH and RSDH levels are presented in Table S13 and compared against experimental values. It is noted that all DH and RSDH functionals are not able to predict the shifts for BODIPY compounds in a reasonable way. The MAE values of all functionals are relatively high, and their linear determination coefficient values R^2 are around 0.5 eV or much lower. For instance, the MAE values of the two DSD functionals are around 0.15 eV, and R^2 values are around 0.05 eV (Table S13). Although the performance of the two range separated DH functionals is slightly better than that of two DSDs, e.g. MAE around 0.1 eV and R^2 around 0.5 eV, their predictive power is obviously still very poor.

4. Conclusions

Most TD-DFT functionals investigated in this work are found to overestimates the calculated vertical excitation energies by more than 0.4 eV in general for the set of BODIPY compounds studied in this work. The MAE values of GGA functionals ($\approx$ 0.26 eV), however, are found to be in the regular range of errors typically acceptable for TD-DFT functionals ($<$ 0.3 eV). The GH-GGA, GH-mGGA, RSH-GGA, RSDH-GGA and some DH-GGA functionals are not recommended for TD-DFT calculations on BODIPY molecular systems. Furthermore, the performance of GH-GGA and GH-mGGA functionals is found to deteriorate with increasing the percentage of the HF exchange.

The MAE values of the two dispersion-corrected, spin-component-scaled, double-hybrid (DSD) functionals, DSD-BLYP and DSD-PBEP86 were found to be 0.119 eV and 0.124 eV, respectively. The performance of these two "semiemperical" DH functionals is therefore close to the desired chemical accuracy ($\lesssim$0.1 eV) for an excited state method, and in the same range of errors that was reported for more expensive wavefunction based *ab initio* methods such as LCC2*, SAC-CI, DLPNO-STEOM-CCSD, and CASPT2 [27,38]. In addition, the two DSD functionals tested in this study shows the best relative maximum error and standard deviation among all 36 functionals, and a good linear determination coefficient R^2 (0.933 eV for DSD-BLYP and 0.917 eV for DSD-PBEP86). Hence, the two DSD functionals used in the study are recommended to be used for TD excited state calculations for their accuracy and efficiency.

The performance of DSD-BLYP and DSD-PBEP86 is equally

promising for vertical fluorescence, but reproduce bad predictions of Stokes shifts. In fact, no other DH functional used in this study perform well for the Stokes shifts. We finally recommend to use the linear response LR-CPCM solvation model as it produce a slight improvement in terms of consistency and predictability over gas phase calculations, in particular using the two DH DSD-BLYP and DSD-PBEP86 functionals.

Hopefully, the conclusions of this study will encourage further future investigations in two directions. First, expand the set of BODIPY molecules benchmarked to include new compounds of larger extended size, a wide diversity of molecular configurations, and some new cyanine-like chromophores other than BODIPY compounds. Second, expand the set of DH functionals in general, and the DSDs in particular, in order to be tested on these interesting but "tricky" chemical photo-systems.

Declaration of Competing Interest

The authors declare that they have no known competing financial interests or personal relationships that could have appeared to influence the work reported in this paper.

Acknowledgment

Financial support of this work by the Deanship of Scientific Research at the University of Jordan is gratefully acknowledged. We also thank the reviewers for insightful comments and suggestions.

Appendix A. Supplementary material

Supplementary data associated with this article can be found, in the online version, at https://doi.org/10.1016/j.comptc.2021.113531.

References

[1] Aurore Loudet, Kevin Burgess, Bodipy dyes and their derivatives: Syntheses and spectroscopic properties, Chem. Rev. 107 (11) (2007) 4891–4932.
[2] Alexander B. Nepomnyashchii, Allen J. Bard, Electrochemistry and electrogenerated chemiluminescence of bodipy dyes, Acc. Chem. Res. 45 (11) (2012) 1844–1853. PMID: 22515199.
[3] Jorge Bañuelos, Bodipy dye, the most versatile fluorophore ever? The Chemical Record 16 (1) (2016) 335–348.
[4] Andre Bessette, Garry S. Hanan, Design, synthesis and photophysical studies of dipyrromethene-based materials: insights into their applications in organic photovoltaic devices, Chem. Soc. Rev. 43 (2014) 3342–3405.
[5] Lu. Hua, John Mack, Yongchao Yang, Zhen Shen, Structural modification strategies for the rational design of red/nir region bodipys, Chem. Soc. Rev. 43 (2014) 4778–4823.
[6] Yuan Ge, Donal F. O'Shea, Azadipyrromethenes: from traditional dye chemistry to leading edge applications, Chem. Soc. Rev. 45 (2016) 3846–3864.
[7] Lakshmi Vellanki, Ritambhara Sharma, Mangalampalli Ravikanth, Functionalized boron-dipyrromethenes and their applications, Reports in Organic Chemistry 6 (2016) 1–24.
[8] Raymond Ziessel, Anthony Harriman, Artificial light-harvesting antennae: electronic energy transfer by way of molecular funnels, Chem. Commun. 47 (2011) 611–631.
[9] Surya Prakash Singh, Thumuganti Gayathri, Evolution of bodipy dyes as potential sensitizers for dye-sensitized solar cells, Eur. J. Org. Chem. 2014 (22) (2014) 4689–4707.
[10] Mao Mao, Qin-Hua Song, The structure-property relationships of d-π-a bodipy dyes for dye-sensitized solar cells, The Chemical Record 16 (2) (2016) 719–733.
[11] Hafsah Klfout, Adam Stewart, Mahmoud Elkhalifa, Hongshan He, Bodipys for dye-sensitized solar cells, ACS Applied Materials & Interfaces 9 (46) (2017) 39873–39889. PMID: 29072443.
[12] Haizhen Liu, Liping Liu, Fu. Yan, Erbao Liu, Bingchun Xue, Theoretical design of d–π–a–a sensitizers with narrow band gap and broad spectral response based on boron dipyrromethene for dye-sensitized solar cells, J. Chem. Inf. Model. 59 (5) (2019) 2248–2256. PMID: 30908031.
[13] Yasuhiro Kubota, Kosei Kimura, Jiye Jin, Kazuhiro Manseki, Kazumasa Funabiki, Masaki Matsui, Synthesis of near-infrared absorbing and fluorescing thiophene-fused bodipy dyes with strong electron-donating groups and their application in dye-sensitised solar cells, New J. Chem. 43 (2019) 1156–1165.
[14] Yuta Higashino, Sule Erten-Ela, Yuji Kubo, π-expanded dibenzo-bodipy with near-infrared light absorption: Investigation of photosensitizing properties of nio-based p-type dye-sensitized solar cells, Dyes Pigm. 170 (2019) 107613.
[15] Elif Akhuseyin Yildiz, H. Gokhan Sevinc, Gul Yaglioglu, Mustafa Hayvali, Strategies towards enhancing the efficiency of bodipy dyes in dye sensitized solar cells, J. Photochem. Photobiol., A 375 (2019) 148–157.
[16] Elif Akhuseyin Yildiz, H. Gokhan Sevinc, Gul Yaglioglu, Mustafa Hayvali, The effect of molecular structure and ultrafast electron injection dynamics on the efficiency of bodipy sensitized solar cells, Opt. Mater. 91 (2019) 50–57.
[17] Antonio Aguiar, Joana Farinhas, Wanderson da Silva, Mariana Emilia Ghica, Christopher M.A. Brett, Jorge Morgado, and Abrilio J.F.N. Sobral. Synthesis, characterization and application of meso-substituted fluorinated boron dipyrromethenes (bodipys) with different styryl groups in organic photovoltaic cells. Dyes and Pigments, 168:103–110, 2019.
[18] Gayathri Thumuganti, Vinay Gupta, Surya Prakash Singh, New dithienosilole- and dithienogermole-based bodipy for solar cell applications, New J. Chem. 43 (2019) 8735–8740.
[19] Jian Yang, Charles H. Devillers, Paul Fleurat-Lessard, Hao Jiang, Shifa Wang, Claude P. Gros, Gaurav Gupta, Ganesh D. Sharma, Xu. Haijun, Carbazole-based green and blue-bodipy dyads and triads as donors for bulk heterojunction organic solar cells, Dalton Trans. 49 (2020) 5606–5617.
[20] Alejandro Ortiz, Triarylamine-bodipy derivatives: A promising building block as hole transporting materials for efficient perovskite solar cells, Dyes Pigm. 171 (2019) 107690.
[21] Madhurima Poddar, Rajneesh Misra, Recent advances of bodipy based derivatives for optoelectronic applications, Coord. Chem. Rev. 421 (2020) 213462.
[22] Benedetta Maria Squeo, Mariacecilia (Pasini), Bodipy platform: a tunable tool for green to nir oleds, Supramol. Chem. 32 (1) (2020) 56–70.
[23] Mengdi Liu, Siyue Ma, Mengyao She, Jiao Chen, Zhaohui Wang, Ping Liu, Shengyong Zhang, and Jianli Li. Structural modification of bodipy: Improve its applicability. Chinese Chemical Letters, 30(10):1815–1824, 2019. SI: Fluorescence Basics and Technology.
[24] Abdurrahman Turksoy, Deniz Yildiz, and Engin U. Akkaya. Photosensitization and controlled photosensitization with bodipy dyes. Coordination Chemistry Reviews, 379:47–64, 2019. Novel and Smart Photosensitizers from Molecule to Nanoparticle.
[25] Jian Yang, Hao Jiang, Nicolas Desbois, Guoliang Zhu, Claude P. Gros, Yuanyuan Fang, Frédéric Bolze, Shifa Wang, Xu. Hai-Jun, Synthesis, spectroscopic characterization, one and two-photon absorption properties, and electrochemistry of truxene π-expanded bodipys dyes, Dyes Pigm. 176 (2020) 108183.
[26] Boris Le Guennic, Olivier Maury, Denis Jacquemin, Aza-boron-dipyrromethene dyes: Td-dft benchmarks, spectral analysis and design of original near-ir structures, Phys. Chem. Chem. Phys. 14 (2012) 157–164.
[27] Mohammad R. Momeni, Alex Brown, Why do td-dft excitation energies of bodipy/aza-bodipy families largely deviate from experiment? answers from electron correlated and multireference methods, J. Chem. Theory Comput. 11 (6) (2015) 2619–2632.
[28] Siwar Chibani, Boris Le Guennic, Azzam Charaf-Eddin, Olivier Maury, Chantal Andraud, Denis Jacquemin, On the computation of adiabatic energies in aza-boron-dipyrromethene dyes, J. Chem. Theory Comput. 8 (9) (2012) 3303–3313.
[29] Siwar Chibani, Boris Le Guennic, Azzam Charaf-Eddin, Adele D. Laurent, Denis Jacquemin, Revisiting the optical signatures of bodipy with ab initio tools, Chem. Sci. 4 (2013) 1950–1963.
[30] Siwar Chibani, Azzam Charaf-Eddin, Benedetta Mennucci, Boris Le Guennic, Denis Jacquemin, Optical signatures of obo fluorophores: A theoretical analysis, J. Chem. Theory Comput. 10 (2) (2014) 805–815. PMID: 26580054.
[31] Siwar Chibani, Adele D. Laurent, Boris Le Guennic, Denis Jacquemin, Improving the accuracy of excited-state simulations of bodipy and aza-bodipy dyes with a joint sos-cis(d) and td-dft approach, J. Chem. Theory Comput. 10 (10) (2014) 4574–4582. PMID: 26588151.
[32] Azzam Charaf-Eddin, Boris Le Guennic, Denis Jacquemin, Excited-states of bodipy-cyanines: ultimate td-dft challenges? RSC Adv. 4 (2014) 49449–49456.
[33] Boris Le Guennic, Denis Jacquemin, Taking up the cyanine challenge with quantum tools, Acc. Chem. Res. 48 (3) (2015) 530–537.
[34] Paul Boulanger, Siwar Chibani, Boris Le Guennic, Ivan Duchemin, Xavier Blase, Denis Jacquemin, Combining the bethe-salpeter formalism with time-dependent dft excited-state forces to describe optical signatures: Nbo fluoroborates as working examples, J. Chem. Theory Comput. 10 (10) (2014) 4548–4556. PMID: 26588148.
[35] Ou. Qi, Qian Peng, Zhigang Shuai, Toward quantitative prediction of fluorescence quantum efficiency by combining direct vibrational conversion and surface crossing: Bodipys as an example, The Journal of Physical Chemistry Letters 11 (18) (2020) 7790–7797. PMID: 32787317.
[36] I.K. Petrushenko, K.B. Petrushenko, Effect of meso-substituents on the electronic transitions of bodipy dyes: Dft and ri-cc2 study, Spectrochim. Acta Part A Mol. Biomol. Spectrosc. 138 (2015) 623–627.
[37] Flip de Jong, Milica Feldt, Jonas Feldt, Jeremy N. Harvey, Modelling absorption and emission of a meso-aniline-bodipy based dye with molecular mechanics, Phys. Chem. Chem. Phys. 20 (2018) 14537–14544.
[38] Milica Feldt, Alex Brown, Assessment of local coupled cluster methods for excited states of bodipy/aza-bodipy families, J. Comput. Chem. 42 (3) (2021) 144–155.
[39] Romain Berraud-Pache, Frank Neese, Giovanni Bistoni, Robert Izsak, Computational design of near-infrared fluorescent organic dyes using an accurate new wave function approach, The Journal of Physical Chemistry Letters 10 (17) (2019) 4822–4828. PMID: 31386375.
[40] Romain Berraud-Pache, Frank Neese, Giovanni Bistoni, Róbert Izsák, Unveiling the photophysical properties of boron-dipyrromethene dyes using a new accurate excited state coupled cluster method, J. Chem. Theory Comput. 16 (1) (2020) 564–575. PMID: 31765141.

[41] Stefan Grimme, Frank Neese, Double-hybrid density functional theory for excited electronic states of molecules, J. Chem. Phys. 127 (15) (2007) 154116.

[42] Barry Moore, Jochen Autschbach, Longest-wavelength electronic excitations of linear cyanines: The role of electron delocalization and of approximations in time-dependent density functional theory, J. Chem. Theory Comput. 9 (11) (2013) 4991–5003. PMID: 26583416.

[43] Timothy J. Lee, Peter R. Taylor, A diagnostic for determining the quality of single-reference electron correlation methods, Int. J. Quantum Chem. 36 (S23) (1989) 199–207.

[44] Amir Karton, Elena Rabinovich, Jan M.L. Martin, and Branko Ruscic. W4 theory for computational thermochemistry: In pursuit of confident sub-kj/mol predictions. The Journal of Chemical Physics, 125(14):144108, 2006.

[45] R.R. Valiev, A.N. Sinelnikov, Y.V. Aksenova, R.T. Kuznetsova, M.B. Berezin, A. S. Semeikin, V.N. Cherepanov, The computational and experimental investigations of photophysical and spectroscopic properties of bf2 dipyrromethene complexes, Spectrochim. Acta Part A Mol. Biomol. Spectrosc. 117 (2014) 323–329.

[46] Stefan Grimme, Semiempirical hybrid density functional with perturbative second-order correlation, J. Chem. Phys. 124 (3) (2006) 034108.

[47] Lars Goerigk, Stefan Grimme, Double-hybrid density functionals, WIREs Computational Molecular Science 4 (6) (2014) 576–600.

[48] Jan M.L. Martin, Golokesh Santra, Empirical double-hybrid density functional theory: A 'third way' in between wft and dft, Isr. J. Chem. 60 (8–9) (2020) 787–804.

[49] Lars Goerigk, Jonas Moellmann, Stefan Grimme, Computation of accurate excitation energies for large organic molecules with double-hybrid density functionals, Phys. Chem. Chem. Phys. 11 (2009) 4611–4620.

[50] Lars Goerigk, Stefan Grimme, Double-hybrid density functionals provide a balanced description of excited 1la and 1lb states in polycyclic aromatic hydrocarbons, J. Chem. Theory Comput. 7 (10) (2011) 3272–3277. PMID: 26598161.

[51] Tobias Schwabe, Lars Goerigk, Time-dependent double-hybrid density functionals with spin-component and spin-opposite scaling, J. Chem. Theory Comput. 13 (9) (2017) 4307–4323. PMID: 28763220.

[52] Marcos Casanova-Páez, Michael B. Dardis, Lars Goerigk, ωb2plyp and ωb2g pplyp: The first two double-hybrid density functionals with long-range correction optimized for excitation energies, J. Chem. Theory Comput. 15 (9) (2019) 4735–4744. PMID: 31298850.

[53] Eric Bremond, Marika Savarese, Angel Jose Perez-Jimenez, Juan Carlos Sancho-Garcia, and Carlo Adamo. Speed-up of the excited-state benchmarking: Double-hybrid density functionals as test cases. Journal of Chemical Theory and Computation, 13(11), 5539–5551, 2017.

[54] Alistar Ottochian, Carmela Morgillo, Ilaria Ciofini, Michael J. Frisch, Giovanni Scalmani, Carlo Adamo, Double hybrids and time-dependent density functional theory: An implementation and benchmark on charge transfer excited states, J. Comput. Chem. 41 (13) (2020) 1242–1251.

[55] Amir Karton, Alex Tarnopolsky, Jean-François Lamère, George C. Schatz, Jan M. L. Martin, Highly accurate first-principles benchmark data sets for the parametrization and validation of density functional and other approximate methods. derivation of a robust, generally applicable, double-hybrid functional for thermochemistry and thermochemical kinetics, The Journal of Physical Chemistry A 112 (50) (2008) 12868–12886.

[56] Tobias Schwabe, Stefan Grimme, Towards chemical accuracy for the thermodynamics of large molecules: new hybrid density functionals including non-local correlation effects, Phys. Chem. Chem. Phys. 8 (2006) 4398–4401.

[57] Sebastian Kozuch, David Gruzman, Jan M.L. Martin, Dsd-blyp: A general purpose double hybrid density functional including spin component scaling and dispersion correction, The Journal of Physical Chemistry C 114 (48) (2010) 20801–20808.

[58] Sebastian Kozuch, Jan M.L. Martin, Dsd-pbep86: in search of the best double-hybrid dft with spin-component scaled mp2 and dispersion corrections, Phys. Chem. Chem. Phys. 13 (2011) 20104–20107.

[59] Frank Neese, The orca program system, WIREs Computational Molecular Science 2 (1) (2012) 73–78.

[60] Frank Neese, Software update: the orca program system, version 4.0, WIREs Computational Molecular Science 8 (1) (2018) e1327.

[61] Abdul-Rahman Allouche, Gabedit—a graphical user interface for computational chemistry softwares, J. Comput. Chem. 32 (1) (2011) 174–182.

[62] Carlo Adamo, Vincenzo Barone, Toward reliable density functional methods without adjustable parameters: The pbe0 model, J. Chem. Phys. 110 (13) (1999) 6158–6170.

[63] Florian Weigend, Reinhart Ahlrichs, Balanced basis sets of split valence, triple zeta valence and quadruple zeta valence quality for h to rn: Design and assessment of accuracy, Phys. Chem. Chem. Phys. 7 (2005) 3297–3305.

[64] Denis Jacquemin, Aurelien Planchat, Carlo Adamo, Benedetta Mennucci, Td-dft assessment of functionals for optical 0–0 transitions in solvated dyes, J. Chem. Theory Comput. 8 (7) (2012) 2359–2372. PMID: 26588969.

[65] Denis Jacquemin, Valérie Wathelet, Eric A. Perpète, Carlo Adamo, Extensive td-dft benchmark: Singlet-excited states of organic molecules, J. Chem. Theory Comput. 5 (9) (2009) 2420–2435. PMID: 26616623.

[66] Vincenzo Barone, Maurizio Cossi, Quantum calculation of molecular energies and energy gradients in solution by a conductor solvent model, The Journal of Physical Chemistry A 102 (11) (1998) 1995–2001.

[67] Róbert Izsák, Frank Neese, An overlap fitted chain of spheres exchange method, J. Chem. Phys. 135 (14) (2011) 144105.

[68] Frank Neese, Frank Wennmohs, Andreas Hansen, and Ute Becker. Efficient, approximate and parallel hartree-fock and hybrid dft calculations. a 'chain-of-spheres' algorithm for the hartree-fock exchange. Chemical Physics, 356(1): 98–109, 2009. Moving Frontiers in Quantum Chemistry.

[69] Florian Weigend, Marco Häser, Holger Patzelt, Reinhart Ahlrichs, Ri-mp2: optimized auxiliary basis sets and demonstration of efficiency, Chem. Phys. Lett. 294 (1) (1998) 143–152.

[70] Florian Weigend, Accurate coulomb-fitting basis sets for h to rn, Phys. Chem. Chem. Phys. 8 (2006) 1057–1065.

[71] Arnim Hellweg, Christof Hättig, Sebastian Höfener, Wim Klopper, Optimized accurate auxiliary basis sets for ri-mp2 and ri-cc2 calculations for the atoms rb to rn, Theoret. Chem. Acc. 117 (2007) 587–597.

[72] Oliver Treutler, Reinhart Ahlrichs, Efficient molecular numerical integration schemes, J. Chem. Phys. 102 (1) (1995) 346–354.

[73] Aleksandr V. Marenich, Christopher J. Cramer, Donald G. Truhlar, Ciro A. Guido, Benedetta Mennucci, Giovanni Scalmani, Michael J. Frisch, Practical computation of electronic excitation in solution: vertical excitation model, Chem. Sci. 2 (2011) 2143–2161.

[74] Siwar Chibani, Azzam Charaf-Eddin, Boris Le Guennic, Denis Jacquemin, Boranil and related nbo dyes: Insights from theory, J. Chem. Theory Comput. 9 (7) (2013) 3127–3135. PMID: 26583992.

[75] Pierre-François Loos, Anthony Scemama, Denis Jacquemin, The quest for highly accurate excitation energies: A computational perspective, The Journal of Physical Chemistry Letters 11 (6) (2020) 2374–2383. PMID: 32125872.

[76] Ismael J. Arroyo, Hu. Rongrong, Gabriel Merino, Ben Zhong Tang, and Eduardo Peña-Cabrera. The smallest and one of the brightest. efficient preparation and optical description of the parent borondipyrromethene system, The Journal of Organic Chemistry 74 (15) (2009) 5719–5722. PMID: 19572588.

[77] Timothy W. Ross, Govindarao Sathyamoorthi, Joseph H. Boyer, Biimidazol-2-yl–bf2 complexes, Heteroat. Chem. 4 (6) (1993) 609–612.

[78] Jorge Banuelos, Fernando Lopez Arbeloa, Virginia Martinez, Marta Liras, Angel Costela, Inmaculada Garcia Moreno, and Inigo Lopez Arbeloa. Difluoro-boron-triaza-anthracene: a laser dye in the blue region. theoretical simulation of alternative difluoro-boron-diaza-aromatic systems. Phys. Chem. Chem. Phys., 13: 3437–3445, 2011.

[79] Wu. Liangxing, Kevin Burgess, Syntheses of highly fluorescent gfp-chromophore analogues, J. Am. Chem. Soc. 130 (12) (2008) 4089–4096. PMID: 18321105.

[80] Mikhail S. Baranov, Konstantin A. Lukyanov, Alexandra O. Borissova, Jordan Shamir, Dmytro Kosenkov, Lyudmila V. Slipchenko, Laren M. Tolbert, Ilia V. Yampolsky, Kyril M. Solntsev, Conformationally locked chromophores as models of excited-state proton transfer in fluorescent proteins, J. Am. Chem. Soc. 134 (13) (2012) 6025–6032. PMID: 22404323.

[81] Carlos A. Osorio-Martinez, Arlette Urias-Benavides, C.F. Azael Gomez-Duran, Jorge Banuelos, Ixone Esnal, Inigo Lopez Arbeloa, and Eduardo Pena-Cabrera. 8-aminobodipys: Cyanines or hemicyanines? the effect of the coplanarity of the amino group on their optical properties. The Journal of Organic Chemistry, 77 (12), 5434–5438, 2012.

[82] Govindaro Sathyamoorthi, Joseph H. Boyer, Toomas H. Allik, Suresh Chandra, Laser active cyanopyrromethene-bf2 complexes, Heteroat. Chem. 5 (4) (1994) 403–407.

[83] Yasuhiro Kubota, Toshihiro Tsuzuki, Kazumasa Funabiki, Masahiro Ebihara, Masaki Matsui, Synthesis and fluorescence properties of a pyridomethene–bf2 complex, Org. Lett. 12 (18) (2010) 4010–4013. PMID: 20726588.

[84] Raymond Ziessel, Christine Goze, Gilles Ulrich, Design and synthesis of alkyne-substituted boron in dipyrromethene frameworks, Synthesis 2007 (06) (2007) 936–949.

[85] Thirumani Venkateshwar Goud, Ahmet Tutar, Jean-Francois Biellmann, Synthesis of 8-heteroatom-substituted 4,4-difluoro-4-bora-3a,4a-diaza-s-indacene dyes (bodipy), Tetrahedron 62 (21) (2006) 5084–5091.

[86] Joseph H. Boyer, Anthony M. Haag, Govindarao Sathyamoorthi, Mou-Ling Soong, Kannappan Thangaraj, Theodore G. Pavlopoulos, Pyrromethene–bf2 complexes as laser dyes: 2, Heteroat. Chem. 4 (1) (1993) 39–49.

[87] Chengteh Lee, Weitao Yang, Robert G. Parr, Development of the colle-salvetti correlation-energy formula into a functional of the electron density, Phys. Rev. B 37 (Jan 1988) 785–789.

[88] Nicholas C. Handy, Aron J. Cohen, Left-right correlation energy, Mol. Phys. 99 (5) (2001) 403–412.

[89] A.D. Becke, Density-functional exchange-energy approximation with correct asymptotic behavior, Phys. Rev. A 38 (Sep 1988) 3098–3100.

[90] John P. Perdew, Density-functional approximation for the correlation energy of the inhomogeneous electron gas, Phys. Rev. B 33 (Jun 1986) 8822–8824.

[91] Xu. Xin, William A. Goddard, The x3lyp extended density functional for accurate descriptions of nonbond interactions, spin states, and thermochemical properties, Proc. Nat. Acad. Sci. 101 (9) (2004) 2673–2677.

[92] John P. Perdew, Kieron Burke, Matthias Ernzerhof, Generalized gradient approximation made simple, Phys. Rev. Lett. 77 (Oct 1996) 3865–3868.

[93] Carlo Adamo, Vincenzo Barone, Exchange functionals with improved long-range behavior and adiabatic connection methods without adjustable parameters: The mpw and mpw1pw models, J. Chem. Phys. 108 (2) (1998) 664–675.

[94] Stefan Grimme, Stephan Ehrlich, Lars Goerigk, Effect of the damping function in dispersion corrected density functional theory, J. Comput. Chem. 32 (7) (2011) 1456–1465.

[95] Yan Zhao, Donald G. Truhlar, A new local density functional for main-group thermochemistry, transition metal bonding, thermochemical kinetics, and noncovalent interactions, J. Chem. Phys. 125 (19) (2006) 194101.

[96] Jianmin Tao, John P. Perdew, Viktor N. Staroverov, Gustavo E. Scuseria, Climbing the density functional ladder: Nonempirical meta–generalized gradient approximation designed for molecules and solids, Phys. Rev. Lett. 91 (Sep 2003) 146401.
[97] Axel D. Becke, Density-functional thermochemistry. iii. the role of exact exchange, J. Chem. Phys. 98 (7) (1993) 5648–5652.
[98] P.J. Stephens, F.J. Devlin, C.F. Chabalowski, M.J. Frisch, Ab initio calculation of vibrational absorption and circular dichroism spectra using density functional force fields, The Journal of Physical Chemistry 98 (45) (1994) 11623–11627.
[99] Axel D. Becke, A new mixing of hartree-fock and local density-functional theories, J. Chem. Phys. 98 (2) (1993) 1372–1377.
[100] Viktor N. Staroverov, Gustavo E. Scuseria, Jianmin Tao, John P. Perdew, Comparative assessment of a new nonempirical density functional: Molecules and hydrogen-bonded complexes, J. Chem. Phys. 119 (23) (2003) 12129–12137.
[101] Stefan Grimme, Accurate calculation of the heats of formation for large main group compounds with spin-component scaled mp2 methods, The Journal of Physical Chemistry A 109 (13) (2005) 3067–3077. PMID: 16833631.
[102] Yan Zhao, Donald G. Truhlar, The m06 suite of density functionals for main group thermochemistry, thermochemical kinetics, noncovalent interactions, excited states, and transition elements: two new functionals and systematic testing of four m06-class functionals and 12 other functionals, Theoret. Chem. Acc. 120 (1) (2008) 215–241.
[103] Yoshihiro Tawada, Takao Tsuneda, Susumu Yanagisawa, Takeshi Yanai, Kimihiko Hirao, A long-range-corrected time-dependent density functional theory, J. Chem. Phys. 120 (18) (2004) 8425–8433.
[104] Takeshi Yanai, David P Tew, Nicholas C Handy, A new hybrid exchange–correlation functional using the coulomb-attenuating method (cam-b3lyp), Chem. Phys. Lett. 393 (1) (2004) 51–57.
[105] Jeng-Da Chai, Martin Head-Gordon, Systematic optimization of long-range corrected hybrid density functionals, J. Chem. Phys. 128 (8) (2008) 084106.
[106] You-Sheng Lin, Guan-De Li, Shan-Ping Mao, Jeng-Da Chai, Long-range corrected hybrid density functionals with improved dispersion corrections, J. Chem. Theory Comput. 9 (1) (2013) 263–272.
[107] Asim Najibi, Lars Goerigk, The nonlocal kernel in van der waals density functionals as an additive correction: An extensive analysis with special emphasis on the b97m–v and ωb97m-v approaches, J. Chem. Theory Comput. 14 (11) (2018) 5725–5738.
[108] Narbe Mardirossian, Martin Head-Gordon, ωb97x-v: A 10-parameter, range-separated hybrid, generalized gradient approximation density functional with nonlocal correlation, designed by a survival-of-the-fittest strategy, Phys. Chem. Chem. Phys. 16 (2014) 9904–9924.